A MODEL OF HORIZONTAL TAILPLANE DAMAGE FOR USE IN FLIGHT DYNAMICS

Nicolas Fezans, Carsten Kappenberger
German Aerospace Center (DLR) - Institute of Flight Systems
nicolas.fezans@dlr.de; carsten.kappenberger@dlr.de

Keywords: *Damaged aircraft, two-parts model, flight dynamics, empennage damage modeling*

Abstract

In this paper, an extension of an airplane flight dynamics model structure originally developed for the needs of airplane identification is proposed. The aim of this extension is to separate the contributions of the horizontal tailplane (HTP) from the rest of the model in order to ease the integration of HTP damage in the model. To perform this separation the contribution of the HTP must be identified, which is not possible from flight test data (unless unconventional sensors would be used). It is explained how CFD, wind tunnel or handbook methods can support the separation of the HTP contribution as well as how a simple parameterized HTP damage model can be obtained using the lifting line theory. Data from the literature is used to illustrate the accuracy of the simple damage model. 2D-RANS-CFD results are used to illustrate the accuracy of various handbook methods that are suggested for the modelling of the zero lift angle of attack of the HTP.

Nomenclature

Acronyms

HTP	Horizontal Tailplane
VTP	Vertical Tailplane
FMTA	Future Military Transport Aircraft
CFD	Computational Fluid Dynamics
RANS	Reynolds-Averaged Navier Stokes

Symbols

α	Angle of attack
α_0	Zero lift angle of attack
β	Sideslip angle
η_H	HTP trim angle (wrt. fuselage axis)
ε_H	Downwash angle
$\bar{q}$	Dynamic pressure
$(\vec{x}, \vec{y}, \vec{z})$	Body-fixed reference system
$(\vec{x}_a, \vec{y}_a, \vec{z}_a)$	Aerodynamic reference system
P_W	Wing quarter chord point
P_H	HTP quarter chord point
$\overrightarrow{P_H P_W}$	Vector defined by P_H and P_W
G	Center of gravity
$\vec{L}$	Lift force
$\vec{D}$	Drag force
$\vec{M}$	Pitching moment
$\mathcal{C}$	Aircraft configuration
C_L	Lift coefficient
C_{L0}	Lift coefficient at $\alpha = 0$
$C_{L\alpha}$	Lift coefficient α-derivative
C_D	Drag coefficient
C_{D0}	Drag coefficient at $\alpha = 0$
C_m	Pitch coefficient
C_{m0}	Pitch coefficient at $\alpha = 0$
$C_{m\alpha}$	Pitch coefficient α-derivative
C_{mq}	Pitch coefficient q-derivative
$C_{m\dot{\alpha}}$	Pitch coefficient $\dot{\alpha}$-derivative
S_W , S_H	Wing and HTP surfaces
S_L , S_R	Left and right HTP surfaces
l_W , l_H	Wing and HTP reference chords
Λ	Aspect ratio
ϕ	Quarter chord line sweep angle
e	Oswald efficiency factor

Operators

$\cdot$	Scalar product
$\wedge$	Vector (cross) product

Exponents and Indices

W	Wing
WF	Wing-Fuselage
H	Horizontal Tailplane
global	Complete Aircraft
$@\cdot$	$\cdot$ defines the considered moment reference point of the expression

1 Introduction

1.1 Context

Flight safety has been a major concern for the entire industry since the early days of aviation, reaching very high safety levels. However aircraft safety has to be reinvented constantly as new airplanes including new technologies, architectures, or philosophy are being developed. With the very high reliability level reached by aircraft systems and their constantly increasing complexity, human factors stay one of the major variables involved in flight safety. At the German Aerospace Center (DLR) Institute of Flight Systems the work of the Cognetics group focuses on the issues related to human factors for various type of aircraft and in particular for civil transport aircraft.

Military transport aircraft are also topic of this research. The main issues related to civil aircraft are also affecting military aircraft, however some characteristics of military transport aircraft must be treated separately due to specific missions (e.g. airdrop or aerial refueling) and operational conditions (e.g. battle zones). The risk of major damages for military aircraft operating in battle zones is drastically higher than for civil airplanes and cannot always be addressed through increased physical redundancy, even if costs were neglected. At the same time, a new generation of military transport aircraft is being equipped with fly-by-wire control systems, which have been proven on civil airplane during the last decades. These technologies are bringing new possibilities for handling major damages that must be investigated in order to exploit the full potential of the aircraft in the presence of severe damages. These investigations include fault detection and isolation (FDI) and fault tolerant control (FTC) approaches and consider the entire panel of missions as well as the human factors issues. In order to perform these research activities high-quality simulation models that include realistic damage models as well as error handling and propagation in fly-by-wire architectures are required.

In this paper, current modeling activities for various types of structural damage will be discussed with a specific focus on damages affecting aircraft aerodynamics and in particular at the empennage. Flight control systems malfunctions and damage to the landing gears are also being considered, but not in the present paper. These activities are part of the DLR project “MiTraPor II”, which has the objective to develop tools for the evaluation of future military transport aircraft (FMTA) concepts. Within this project and its predecessor several FMTA related research activities are carried out jointly by the DLR Institute of Flight Systems, the DLR Institute of Aerodynamics and Flow Technology, the DLR Institute of Aeroelasticity as well as the German-Dutch Wind Tunnels (DNW).

A simulation model of a future military transport aircraft (FMTA) as a generic four engine turboprop aircraft was developed [1]. An cargo airdrop simulation [2] was also generated using both this simulation model and the flow field behind the aircraft with open rear door. The aerodynamic model of the FMTA is extended in the current work to include the effects resulting from structural damage. A motivation for the development of this extended model is to support authors’ research activities on fault detection and isolation techniques, on robust / reconfigurable flight control systems, as well as on the human factor issues in faulty conditions.

1.2 Damaged Aircraft Modeling

The current activities regarding the development of damage models within the MiTraPor II project pursue two main objectives: obtaining a simple and real-time capable flight dynamics model of acceptable quality as well as developing and demonstrating the capabilities of various techniques and tools (from Fault Detection, Isolation and Reconfiguration algorithm to CFD). "Acceptable quality" in this context is defined as a quality of the model that makes inaccuracies unnoticeable to the pilot, even if he was flying both the real aircraft and the modeled aircraft one after the other. This very subjective definition does not permit to formulate objectives as a set of mathematical criteria, but represents better than any other criterion what is really being pursued for the models.

Models of damaged aircraft have been developed at NASA for the Generic Transport aircraft Model (GTM) [3–5]. The damage scenarios were investigated using wind tunnel experiments as well as various CFD solvers. Considered damages were: wing tip loss, Horizontal Tailplane (HTP) tip loss, Vertical Tailplane (VTP) tip loss, Elevator off, Rudder off, a hole in the wing and a hole in the HTP. For each of the "tip loss" cases various levels were considered depending on the proportion of the semispan that is missing (with respect to the undamaged semispan). Some of these cases were integrated in the GTM simulation model using MATLAB/Simulink.

In [6] the "hole in the wing" case was also investigated for a NACA 64_1-412 airfoil using the commercial software package Fluent and the numerical results are compared to a wind tunnel experiment.

Many other CFD techniques (e.g. strip methods, vortex lattice methods (VLM), doublet lattice methods (DLM), panel methods) provide interesting trade-offs between derivative models and handbook methods on one side and RANS-CFD techniques on the other side. These techniques can be good alternatives to RANS-CFD in many applications and in particular can also provide good estimates of local forces and moments without their computational cost. These local forces and moments are particularly interesting when considering loads and can only very roughly be provided by derivative models. When considering damage scenarios that do not disturb the "flow quality" too much, the models can be adapted by modifying the aircraft geometry as proposed in [7]. Effects regarding viscosity or flow separation should rather be investigated using Navier-Stokes based CFD and wind tunnel experiments. They are often neglected or modeled in a drastically simplified form for applications requiring short computation time or real-time capability.

Given the aforementioned works, the approach chosen for the damage modeling in the MiTraPor II project is:

- to focus on leading edge damage scenarios
- and to model already investigated empennage damages (tip loss and control surfaces off) using data from the literature, handbook methods and already existing wind tunnel and RANS-CFD data.

Investigations on leading edge damage are outside the scope of this paper but can be found in [8]. Effects of partial leading edge damages on a wing could be observed in the flight recorder data of the El Al flight 1892 (Boeing 747) that crashed on October 4, 1992 at Amsterdam. In this accident, a significant part of the right wing leading edge was damaged during the loss of both engines 3 and 4 (engine 3 pin broke releasing the engine which impacted the leading edge and engine 4). As an effect of this damage, the global $C_{L\alpha}$ of the aircraft was reduced and the lift distribution drastically modified, which led to a rolling moment higher than the ailerons roll authority at low speed. When the pilots reduced the speed to prepare for landing in Amsterdam they lost the control through insufficient roll authority to balance the lift asymmetry between the two wings [9].

In this paper, a way how simple handbook methods and already existing data can support the modeling of HTP damages is presented. Flight

test data do not permit in general (i.e. without unusual sensor configurations) to separate the contribution of the HTP to the aircraft motion, which is a prerequiste for the integration of any HTP damage model. The proposed solution to reconstitute the missing information consist in rewriting slightly the usual two-point model structure and in estimating the zero lift angle of attack of HTP α_0^H. This solution provides good results and is applicable to any airplane flight dynamic model as long as α_0^H is known or can be estimated (in most cases the knowledge of the HTP airfoil will be sufficient for that). Additionally, it remains much simpler than integrating locally forces on CFD results or using wind tunnel tests for various models configurations.

Another requirement for the model is to remain easy to understand for the flight mechanical engineers. Numerical methods such as VLM or DLM are significantly less computationally demanding than RANS-CFD, but still do not really provide the engineers insight into the behavior of the aircraft without performing simulations. Even though the so-called "derivative-models" are primarily designed to perform simulations, they do provide information on the flight dynamic behavior of the aircraft just by looking at the sign of some derivatives or of simple expressions based on them (e.g. on the stability of modes). Therefore, the initial approach is to use so called "derivative-models" and to feed the derivatives with the appropriate information : this type of modeling was found to be accurate enough.

For conciseness only HTP damages and longitudinal equations are considered and discussed hereafter, even though the current activities also consider VTP damage and the six degrees of freedom of a rigid airplane. Note that HTP and VTP should not be modeled independently as they often influence each other. A well-known example is the increased effectiveness of the VTP in a T-tail configuration: in that case the VTP is approximately as effective as it would be if it were having an infinite aspect ratio. The idea of two-points model is extended to include also the lateral dynamics by using so called "two-parts" models where the second part is the complete empennage. This "two-parts" model concept is briefly introduced in this paper, but is completely equivalent to the two-points model concept when only the longitudinal equations are considered, as done hereafter.

2 Two-Points Model Structure

2.1 Origin and Basic Idea

Flight test and aircraft identification have been performed continually at DLR and this for a large variety of aircraft such as: airplanes (e.g. VFW-614 ATTAS, HFB 320, Dornier 328, C-160 Transall, Diamond DA-42, Pitts S-2B, X-31, et al.), helicopters (BO-105, EC-135 ACT/FHS), autogyro (MTO Sport) or even parachutes. These permanent activities led to a set of internal tools, best practices and many derivative models of very good quality. An overview of the methods and models developed can be found in [11].

For identification of airplanes, and in particular of the time-lag effects in their dynamic response, a formulation of longitudinal dynamics showed very good results for all these identification activities. This structure has no commonly recognized name in the community and we will refer to it under the name "two-points model". The two-points model structure has been widely adopted in the flight dynamics community since a long time and is presented in many textbooks [12–17], certainly due to the fact that it represents well the dynamical behavior of airplanes, while being still very simple and therefore suited for explaining and teaching aircraft dynamical behavior.

The basic idea is to model the aircraft wings, fuselage, landing gears, and other parts (for instance rear door) separately from the horizontal tailplane (HTP). The differences in terms of forces and moments on the first part resulting from the presence of the HTP can be neglected and thus be modeled independently. On the contrary, the flow around the HTP strongly depends on the aerodynamics of the first part and especially of the wings. The main effect on the longi-

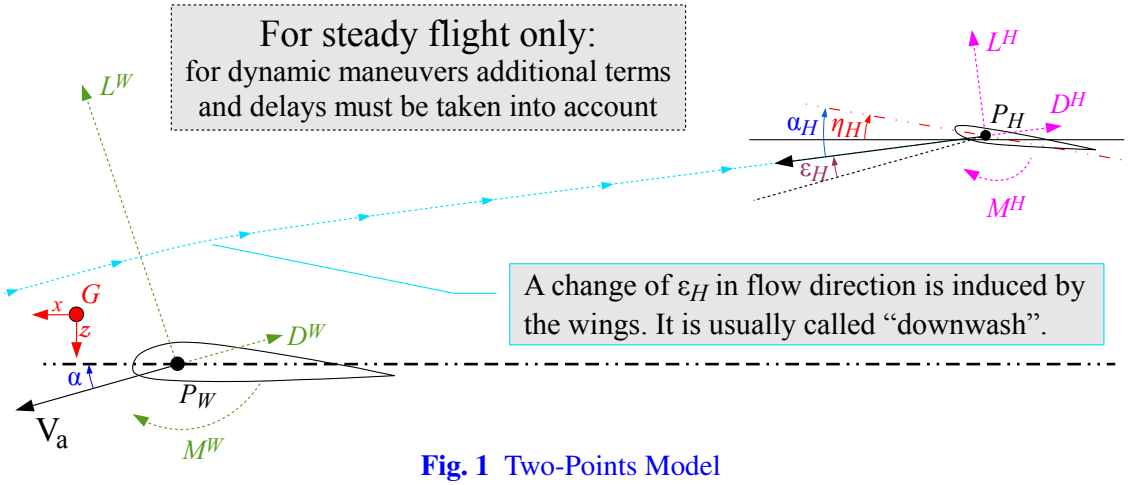

Fig. 1 Two-Points Model

tudinal motion during steady flight can be modeled by a downwash term ε_H, see Fig. 1. This downwash leads to a reduction of the angle of attack at the HTP position and thus to a reduction of the HTP lift (i.e. an additional downforce).

This downwash term strongly depends on the amount of lift generated by the wings and usually this dependence can be well represented by a linear function. As the lift-curve slope is itself an affine function of the angle of attack α in attached flow, the downwash term can be written as:

$$\forall t, \varepsilon_H(t) = \varepsilon_0 + \frac{\partial \varepsilon_H}{\partial \alpha}\ \alpha(t) \qquad (1)$$

with ε_0 and $\partial\varepsilon_H/\partial\alpha$ being constant. Eq. (1) was derived under the implicit assumption that the downwash at the HTP position is immediate. In reality the downwash is generated at the wing position and therefore a delay between downwash generation and encounter of the HTP will occur. This delay corresponds to the time required for the HTP to cover (with respect to the air) the distance separating it from the wings, i.e.: $\tau_\alpha = \overrightarrow{P_H P_W} \cdot \vec{x}_a / V_a \approx |P_W P_H| / V_a$. Finally, Eq. (1) can be rewritten as:

$$\forall t, \varepsilon_H(t) = \varepsilon_0 + \frac{\partial \varepsilon_H}{\partial \alpha}\ \alpha(t - \tau_\alpha) \qquad (2)$$

This delay cannot be taken into account without approximations in a "single-point" model, because it only affects the HTP (ie. the second point). An usual but not very good approximation of this term makes use of the so-called "$\dot{\alpha}$-derivatives". Note that with no change regarding the underlying assumptions, Eq. (2) can be written equivalently:

$$\forall t, \varepsilon_H(t) = \frac{\partial \varepsilon_H}{\partial \alpha}\ (\alpha(t - \tau_\alpha) - \alpha_0) \qquad (3)$$

where α_0 is the angle of attack for which the first part (here just a wing) generates no lift. It seems that there is no consensus regarding the influence of a fuselage on the downwash at HTP position and in particular whether α_0^W or α_0^{WF} should be used in Eq. (3) in that case. The possible error made here would however only slightly affect the static terms and be equivalent to a very limited error on the static trim deflection of the HTP.

In addition to the induced flow field, the inertial speed vectors of the wing quarter chord point P_W and of the HTP quarter chord point P_H are not identical. This is due to the rotational rates p, q, and r and the relative positions of these two points. Considering only the pitch motion, an additional pitch-rate-induced angle of attack at HTP noted α_{dyn}^H must be taken into account as follows:

$$\alpha_{dyn}^H = \arctan\left(\frac{q\ \overrightarrow{P_H P_W} \cdot \vec{x}_a}{V_a}\right) \qquad (4)$$

As α and β are usually relatively small, Eq. (4) is often approximated as follows:

$$\alpha_{dyn}^H \approx \frac{q\ (x_{P_W} - x_{P_H})}{V_a} \qquad (5)$$

The HTP angle of attack can then be expressed as:

$$\alpha_H = \alpha + \eta_H - \varepsilon_H + \alpha_{dyn}^H \qquad (6)$$

which permits to compute the HTP lift and drag forces as well as the pitching moment with respect to the HTP quarter chord point using the HTP derivative model. The same can be made for the other parts of the aircraft model (wing, fuselage, etc.) with respect to another given moment reference point (usually the wing quarter chord point). For the simulation of the equations of motion these forces and moments are both transformed to the aircraft center of gravity and summed. Alternatively, contributions from the different parts can be summed up into global aerodynamic coefficients before computing forces and moments from these coefficients. Of course, both options are equivalent.

2.2 Illustration on a 3D-RANS-CFD result

Before addressing the details of the two-points model structure for the modeling of the interaction between the wing-fuselage and empennage parts, a FMTA 3D-RANS-CFD result with sideslip and without empennage is presented in Fig. 2 to illustrate the physical phenomenon that will be modeled hereafter using a realistic example. This 3D-RANS-CFD computation of the FMTA was performed by the DLR Institute of Aerodynamics and Flow Technology.

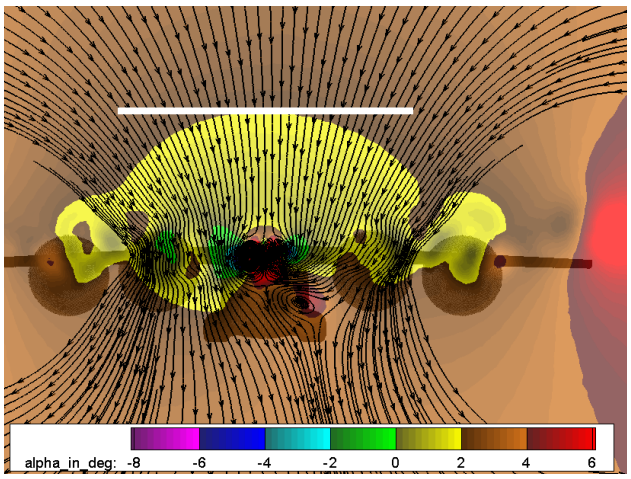

Fig. 2 3D-RANS-CFD Result: "FMTA without empennage, clean configuration, landing gear retracted, rear door closed", $\alpha = 4°$, $\beta = -2°$.

In Fig. 2 the local "α" is represented with the color in a vertical plane located behind the end of the fuselage at the position where the HTP would be. The direction of the (wing-fuselage)-induced velocity components in that plane are shown by the streamlines. The streamlines are therefore not based on the total local velocity components but on the difference between the total ones and the flow at an infinite distance of the aircraft. The downwash and the beginning of the wake vortex formation can easily be observed on the shape of these streamlines. The position where the HTP would be is indicated by the white line. Note that at the HTP position the local α differs significantly from 4°: in the configuration shown the downwash is between 1.5° and 2° downwards. If there was no engine influence and thus if the downwash would be entirely caused by the wing-fuselage aerodynamics, this would corresponds to a $\partial\varepsilon_H/\partial\alpha$ of approximately 0.45. The four turboprop engines were integrated in this CFD computation using rotor discs.

In wind tunnel tests, the flow direction might be directly measured, for instance using particle image velocimetry (PIV) techniques. Often no powered propeller is integrated to the wind tunnel model, so the measured downwash is only the contribution of the wing-fuselage airframe.

Note that the presented CFD result is with a sideslip angle of $-2°$. This type of 3D-RANS-CFD result supports also the modeling of the flow conditions for the VTP. Although the current paper focuses on the HTP part and the longitudinal equations, the current work considers damage scenarios affecting the complete empennage. The idea of the two-points model structure was therefore extended to the six degrees of freedom of the airplane and a separation of the wing-fuselage part and the empennage (HTP+VTP). This extended structure is called two-parts model and is summarized in Fig. 3. $P_{ref,b}$ is a point of the aircraft that can be freely chosen and that serves as reference for the aerodynamic modeling. The green arrow "Induced wind field" is the one-way coupling between the wing-fuselage aerodynamics and the empennage aerodynamics.

Since only the longitudinal equations and the HTP influence are considered in the present paper, it will still be called two-points model. The

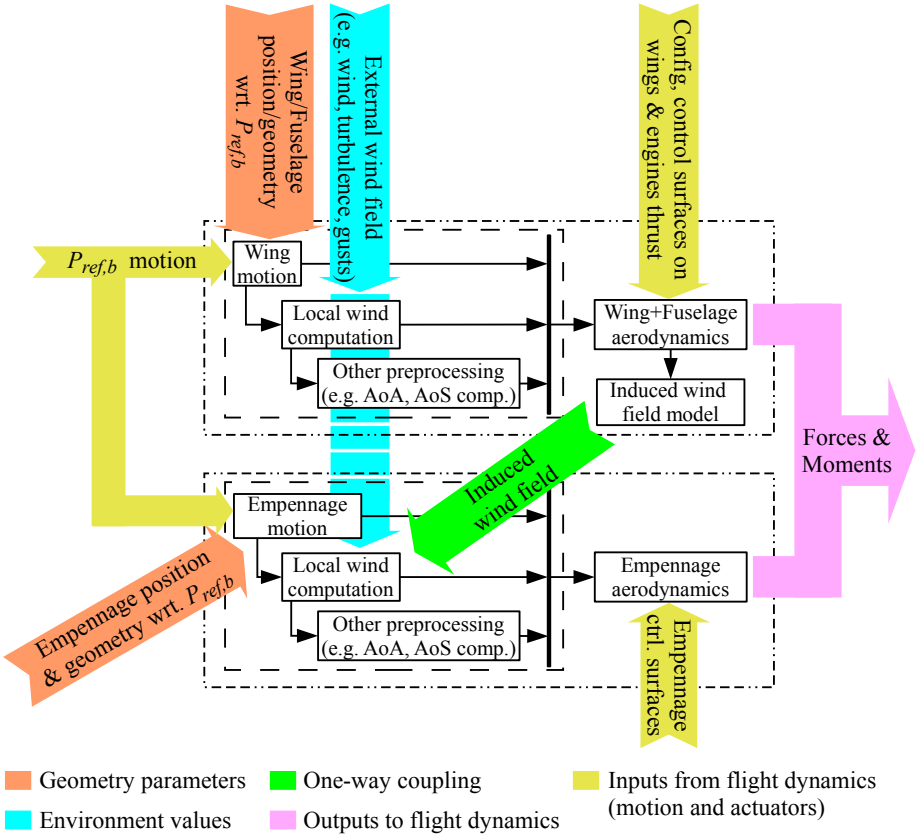

Fig. 3 Two-Parts Model Structure: Wing-Fuselage / Empennage separation

consequences of an asymmetrical damage to the HTP on the lateral dynamic behavior will also not be detailed. For instance, the rolling and yawing moments resulting from the considered HTP damages are not described.

2.3 Equations of the Longitudinal Dynamics

For simplicity, only the main terms (no control surfaces) and for a single configuration will be considered hereafter. For other configurations $\mathcal{C}$ (e.g. slats/flaps), other Mach number or other thrust levels $(T_i)_{i\in[\![1,n]\!]}$ (n being the number of engines) the same equation structure can be used with other numerical values can be set for the wing coefficients. The explicit dependency of the coefficients on all these terms is dropped in the following equations: $C_L(\mathcal{C}, Mach, (T_i)_{i\in[\![1,n]\!]})$ is therefore simply written C_L. Note that the aerodynamic properties of the HTP do not depend on the configuration nor on the thrust levels, however the downwash does. Terms related to the stall model are also dropped for simplicity.

In the following equations the contributions of the wing-fuselage part and of the HTP to the total forces and moments (longitudinal part only) are summed with a global moment reference point at wing quarter chord point P_W. Let $\tilde{\alpha}$ be the angle formed between $\overrightarrow{L}^{WF}$ and $\overrightarrow{L}^{H}$, that is $\tilde{\alpha} = \arccos(\overrightarrow{x_a} \cdot \overrightarrow{x}^{H}_{a}) = \alpha^{H}_{dyn} - \varepsilon_H$.

$$\overrightarrow{L} = \left(L^{WF} + L^{H}\cos\tilde{\alpha} + D^{H}\sin\tilde{\alpha}\right)\frac{\overrightarrow{L}^{WF}}{L^{WF}} \quad (7)$$

$$\overrightarrow{D} = \left(D^{WF} - L^{H}\sin\tilde{\alpha} + D^{H}\cos\tilde{\alpha}\right)\frac{\overrightarrow{D}^{WF}}{D^{WF}} \quad (8)$$

$$\overrightarrow{M}_{@P_W} = \overrightarrow{M}^{WF}_{@P_W} + \overrightarrow{M}^{H}_{@P_H} + \overrightarrow{P_W P_H} \wedge \left(\overrightarrow{L}^{H} + \overrightarrow{D}^{H}\right) \quad (9)$$

The moment at the center of gravity is then obtained as follows:

$$\overrightarrow{M}_{@G} = \overrightarrow{M}_{@P_W} + \overrightarrow{G\,P_W} \wedge \left(\overrightarrow{L} + \overrightarrow{D}\right) \quad (10)$$

The forces and moments used in Eq. (7-9) are computed using the following equations.

$$\overrightarrow{L}^{WF} = -\bar{q}\,S_W\,C_L^{WF}\,\overrightarrow{z}_a \quad (11)$$

$$\overrightarrow{L}^H = -\bar{q}_H \, S_H \, C_L^H \, \overrightarrow{z}_a^H \tag{12}$$

$$\overrightarrow{D}^{WF} = -\bar{q} \, S_W \, C_D^{WF} \, \overrightarrow{x}_a \tag{13}$$

$$\overrightarrow{D}^H = -\bar{q}_H \, S_H \, C_D^H \, \overrightarrow{x}_a^H \tag{14}$$

$$\overrightarrow{M}_{@P_W}^{WF} = \bar{q} \, S_W \, \frac{l_W}{V_a} \, C_m^{WF} \, \overrightarrow{y}_a \tag{15}$$

$$\overrightarrow{M}_{@P_H}^{H} = \bar{q}_H \, S_H \, \frac{l_H}{V_a^H} \, C_m^H \, \overrightarrow{y}_a^H \tag{16}$$

Until this point, the longitudinal equations were derived without any approximation. It was however assumed that the wing-fuselage-induced flow at HTP position is sufficiently homogeneous to define the direction of $\overrightarrow{x}_a^H$. The aerodynamic coefficients used in Eq. (11-16) are computed using the following derivative model equations.

$$C_L^{WF} = C_{L0}^{WF} + C_{L\alpha}^{WF} \, \alpha = C_{L\alpha}^{WF} \, (\alpha - \alpha_0^{WF}) \tag{17}$$

$$C_L^H = C_{L0}^H + C_{L\alpha}^H \, \alpha_H = C_{L\alpha}^H \, (\alpha - \alpha_0^H) \tag{18}$$

$$C_D^{WF} = C_{D0}^{WF} + \frac{(C_L^{WF})^2}{e \, \pi \, \Lambda_W} \tag{19}$$

$$C_D^H = C_{D0}^H + \frac{(C_L^H)^2}{e \, \pi \, \Lambda_H} \tag{20}$$

$$C_{m@P_W}^{WF} = C_{m0@P_W}^{WF} + C_{m\alpha@P_W}^{WF} \, \alpha + C_{mq@P_W}^{WF} \, \frac{q \, l_W}{V_a} \tag{21}$$

$$C_{m@P_W}^{H} = C_{m0@P_W}^{H} + C_{m\alpha@P_W}^{H} \, \alpha_H + C_{mq@P_W}^{H} \, \frac{(q + \dot{\eta}_H) \, l_H}{V_a^H} \tag{22}$$

Additionally, it is usually assumed that $V_a^H = V_a$ and that $\bar{q}_H = \bar{q}$. Note that when considering only the longitudinal dynamics for an aircraft whose wing-fuselage part is symmetrical and without sideslip, the following equation necessarily applies $\overrightarrow{y}_a^H = \overrightarrow{y}_a$.

In practice, for the needs of the flight dynamics models many terms in the equations (7-22) are negligible. For instance, the derivative of the pitching moment of the wing-fuselage configuration with respect to the wing quarter chord point and of the HTP with respect to HTP quarter chord point are very small in comparison to the pitching moment induced by the additional lift at the HTP $\left(\approx S_H/S_W \, |P_W \, P_H|/l_W \, (1 - \partial\varepsilon_H/\partial\alpha) \, C_{L\alpha}^H \right)$. This is due to the relatively small distance between the quarter chord and neutral points for these two parts compared to the distance $|P_W \, P_H|$ between both quarter chord points. The drag of the HTP is important for performance computation but not for the dynamical behavior. The term $D^H \sin\widetilde{\alpha}$ of Eq. (7) can also be dropped.

2.4 Relationship with Single-Point Linear Models

Even though linear models do not represent the airplane dynamics as well as the two-point models do, they are widely used as they permit to use the tools that the linear system theory provides. Besides, they are also good enough for many applications. A two-points model can be converted in a roughly equivalent single-point model by defining the following derivatives:

$$C_{mq@P_W}^{global} = C_{mq@P_W}^{WF} - C_{L\alpha}^H \frac{S_H}{S_W} \, K \tag{23}$$

and

$$C_{m\dot{\alpha}@P_W}^{global} = -C_{L\alpha}^H \frac{S_H}{S_W} \, K \, \frac{\partial\varepsilon_H}{\partial\alpha} \tag{24}$$

with

$$K = \frac{\overrightarrow{P_H P_W} \cdot \overrightarrow{x}_a}{l_W} \, \frac{\overrightarrow{P_H G} \cdot \overrightarrow{x}_a}{l_W} \tag{25}$$

Note that for the derivation of Eq. (23-24), it is additionnally assumed that the angle $\alpha_{dyn}^H - \varepsilon_H$ is small. Note also that single-point models without $\dot{\alpha}$ coefficient derivatives are more commonly used. The $\dot{\alpha}$ derivatives permit to approximate unsteady interaction between wings and HTP instead of neglecting it completely. As working with linear systems offers some advantages, it remains quite common to convert a two-points model into a single-point linear model.

3 Two-Points Model Parameters Values

3.1 Terms that Cannot be Identified From Flight Test

In [10], the use of a two-points model for the identification of the DLR ATTAS research aircraft (VFW-614) was presented. All terms of

the two-points model structure cannot be identified because the terms C_{L0}^{WF}, C_{L0}^{H}, ε_0, and C_{m0}^{WF} are combined in the lift and moment equations in a way such that inertial platform and air data sensor (at the aircraft nose) measurements do not permit to separate their respective contributions afterwards. All other terms can be identified correctly if appropriate maneuvers are flown. Finally, to establish a model of an undamaged aircraft (and without wanting to model damage later) a satisfying solution is to identify the two global terms C_{L0}^{global} and C_{m0}^{global} which result from the four aforementioned ones.

Most of the structural damage scenarios to be modeled affect several aerodynamic coefficient derivatives at a time. However, they do not directly affect the terms C_{L0}^{global} and C_{m0}^{global}, but the subterms C_{L0}^{WF}, C_{L0}^{H}, ε_0, and C_{m0}^{WF}. Consequently, in order to model these damages it is required to proceed to the separation that was not required for the nominal model. This is only possible if additional knowledge or information is available.

Three main sources of information might be considered to enable the separation of these four terms: CFD, wind tunnel, and handbook methods. By reformulating the identification problem using the wing-fuselage zero lift angle of attack α_0^{WF}, it appears that both C_{L0}^{WF} and ε_0 can be substituted with expressions based on α_0^{WF} and parameters that can already be identified in flight test as shown in Eqs. (3) and (17). However three unknowns (α_0^{WF}, C_{L0}^{H}, and C_{m0}^{WF}) involved in the steady state equilibrium of the lift and pitch equations (i.e. only two equations) remain.

As shown in Eq. (18), the parameter C_{L0}^{H} can also be substituted with expressions based on known parameters and the HTP zero lift angle of attack α_0^{H}, which is usually easy to compute using handbook methods.

3.2 Determination of α_0^H

The HTP zero lift angle of attack α_0^H is a parameter that is easy to estimate with good precision using various handbook methods. These handbook methods usually consist of two steps: first, the determination of the airfoil zero lift angle of attack and secondly, the determination of the finite wing zero lift angle of attack using the one of the airfoil and the finite wing geometrical properties. This process is illustrated hereafter using a typical HTP airfoil that is very similar to the FMTA one.

The first method that will be used for this is based on the thin airfoil theory. For an airfoil with a mean camber line described by the function $z(x)$, the zero lift angle α_0 can be computed as follows:

$$\alpha_0 = -\frac{1}{\pi}\int_0^{\pi} \frac{dz}{dx}(\cos\theta_0 - 1)\, d\theta_0 \qquad (26)$$

with $x = c/2\,(1-\cos\theta_0)$ and c the chord length. θ_0 is a term introduced during the derivation of the thin airfoil theory equations using Fourier cosine series expansion. The comprehension of its physical interpretation is not required in order to apply the formula of Eq. (26); it is simply the integration variable and thus a bound variable. The computation is not detailed here but explanations can be found in aerodynamic textbooks and an analytical computation example of the zero lift angle of a NACA 23012 airfoil using the formula of Eq. (26) is detailed in [18].

The two other methods used are also based on the mean camber line of the airfoil. Munk's method [19] is based on Eq. (27) for a normalized airfoil (i.e. dimensions scaled by $1/c$ so that x and z are expressed in fractions of the chord).

$$\alpha_0 = -\sum_{i=1}^{5} k_i\, z(x_i) \qquad (27)$$

The constant coefficients $(k_i)_{i\in[\![1,n]\!]}$ as well as the stations $(x_i)_{i\in[\![1,n]\!]}$ are provided in Table 1.

Table 1 Constants for Munk's Method

x_1	0.99458	k_1	1252.24
x_2	0.87426	k_2	109.048
x_3	0.5	k_3	32.5959
x_4	0.12574	k_4	15.6838
x_5	0.00542	k_5	5.97817

Another approximation is provided by Pankhurst [20] using a similar formula based

Table 2 Constants for Pankhurst's Method

x_1	0	A_1	1.45
x_2	0.025	A_2	2.11
x_3	0.05	A_3	1.56
x_4	0.1	A_4	2.41
x_5	0.2	A_5	2.94
x_6	0.3	A_6	2.88
x_7	0.4	A_7	3.13
x_8	0.5	A_8	3.67
x_9	0.6	A_9	4.69
x_{10}	0.7	A_{10}	6.72
x_{11}	0.8	A_{11}	11.75
x_{12}	0.9	A_{12}	21.72
x_{13}	0.95	A_{13}	99.85
x_{14}	1	A_{14}	-164.9

on 14 stations instead of 5 for Munk's one and placed differently. The formula is provided in Eq. (28) and uses the coordinates of the upper (U) and lower (L) airfoil boundaries. Note that $\forall x,\ U(x)+L(x) = 2\ z(x)$ with $z(x)$ the mean camber line as used previously. Constants are provided in Table 2.

$$\alpha_0 = -\sum_{i=1}^{14} A_i \left(U(x_i)+L(x_i)\right) \qquad (28)$$

The typical HTP airfoil that is used to illustrate the results provided by these methods is a modified and inverted (negative camber) RAE (NLP) 5212 airfoil that is very similar to the FMTA HTP airfoil. This airfoil is represented in Fig. 4. The dashed green line is the airfoil camber line. In addition to the results of the three aforementioned methods the complete airfoil lift curve was available from 2D-RANS-CFD for Mach numbers 0.3 and 0.7, which gives a reference to compare with. All these results are summarized in Table 3. All these values are very close to each

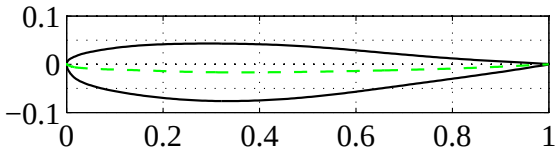

Fig. 4 Modified RAE (NLP) 5212 Airfoil

Table 3 Comparison of Results for α_0 of the airfoil

Method	α_0
2-RANS-CFD @ Mach = 0.3	1.67°
2-RANS-CFD @ Mach = 0.7	1.66°
Pankhurst's method	1.65°
Munk's method	1.61°
Eq. (26)	1.58°

other, which illustrates that these methods provide sufficiently good estimates of airfoil's zero lift angle of attack. Pankhurst's method is closer to the CFD results than the other ones, but this is likely to be of no significance, even though compared to Munk's method this might be due to the higher number of stations considered.

The fact that both CFD results performed at Mach numbers of 0.3 and 0.7 are almost identical also illustrates the fact that there is no dependency on compressibility effects within this range for the airfoil zero lift angle of attack. The flight envelope of the FMTA do not contain Mach numbers for which compressibility effects would be observed, but for most current jet airplanes very significant compressibility effects will be observed in cruise conditions. Note however that for these airplanes and conditions the simple derivative model assumptions (e.g. C_L affine in α) are often invalidated and more complex aerodynamic models should be used.

Once the airfoil zero lift angle of attack is known, the finite wing (in this case the HTP) zero lift angle of attack must still be determined. A known result is that at the zero lift angle of attack of a nontwisted wing based on a single airfoil is the same than the zero lift angle of attack of the airfoil. This is a consequence of the fact that each segment of the wing induces an additional angle of attack at the others only if it generates lift itself: with no twist, a unique airfoil and at airfoil zero lift angle there is no part of the wing generating lift and inducing changes in flow direction for the others. Simple ways to take twist into account in the computation of wing zero lift angle are presented in [14, 21]. For more complex geometries, numerical methods (numerical

lifting line or more complex) will allow to compute the quasi-affine part of lift-curve of the finite wing, from which the zero lift angle of attack of the wing can be deduced. Applying one of the aforementioned methods to the HTP should permit in almost all cases to compute its zero lift angle of attack α_0 with good precision.

3.3 HTP Damage Model

Since the geometry of HTP is usually simple, the determination of its aerodynamic derivatives can be performed using handbook methods. For instance, using the lifting line theory, the HTP lift curve slope coefficient $C^H_{L\alpha}$ can be computed with the equation:

$$C_{L\alpha} = \frac{\pi \Lambda e}{1 + \sqrt{1 + \left(\frac{\pi \Lambda e}{a_\phi}\right)^2 (1 - M_\infty^2 \cos^2 \phi)}} \quad (29)$$

This provides the lift curve slope of a finite wing depending on $a_\phi = a_0 \cos\phi$ (ϕ being the quarter-chord sweep angle and a_0 the airfoil lift curve slope coefficient), on the Mach number M_∞, on the wing aspect ratio Λ, and on the Oswald efficiency factor e. The Oswald efficiency factor can be set to 1 (or slightly less) if no better estimation is known ($e = 1$ corresponds to an elliptical lift distribution). Typical values for e are between 0.6 and 0.9. The lifting line theory usually provides sufficiently good results: to illustrate this, data from [5] were taken and the HTP geometry (sweep angle and aspect ratio) estimated from the top view also shown in this reference in order to be able to recompute the same case using the formula of Eq. (29).

The damage case considered in [5] and recomputed hereafter is a case where a part of the left HTP was lost. The lost part is the tip of the HTP: the nominal HTP was cut parallel to the fuselage's main axis, reducing the semispan of the affected side of the HTP and thus the aspect ratio at least on one side of the aircraft. A tip loss of 25% means that the outer quarter of the left HTP (in terms of semispan) was cut away.

Since the fuselage is between the two halfs of the HTP it seems reasonable to perform the computation using the lifting line method twice (once per side) and each time under the assumption that the other side has the same shape. After that both results are merged using a weighted average based on the respective surfaces S_L and S_R. This operation is summarized by the drawing shown in Fig. 5. The total HTP surface S_H must of course also be computed depending on the damage level: here it would be $S_H = S_L + S_R$.

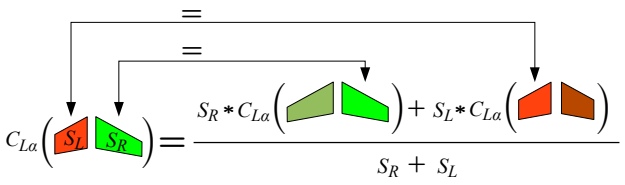

Fig. 5 Weighted Average of the Respective Contributions of the Two HTP Sides.

Data were extracted from the Fig. 4 of [5] with the aim of comparing the prediction of the lifting line theory with these data. This comparison is presented in Fig. 6, where the original data are represented with the blue diamonds. The unknown scaling factor of these data forces us to compare the methods based on the term $\Delta C_{m\alpha}/(C^{WF}_{m\alpha} - C^{\text{global, undamaged}}_{m\alpha})$ instead of directly on the $C_{m\alpha}$. To make these data comparable, the unknown scaling factor was estimated using two of the values contained in the data and was multiplied to the prediction of lifting line theory, i.e. using Eq. (29). The two points used were the cases "no damage" and the case "both sides off". Additionally, in order to illustrate the importance of the variation of the $C^H_{L\alpha}$ induced by the lifting line, the results obtained by keeping the $C^H_{L\alpha}$ constant and adjusting only the surface of the HTP depending on the damage level is also shown in this figure.

Due to the aforementioned estimation of the scaling factor, the point at 0% is the same for all 3 sources. For the lifting line computation, an Oswald factor value of $e = 1$ was used instead of a more realistic value (e.g. 0.8). Therefore the obtained curve should remain below the experimental points. Reason for that, is that the damaged HTP $C^H_{L\alpha}$ will be slightly overestimated for intermediate configurations (neither for 0% nor for

100%, but in between). By keeping the $C_{L\alpha}^{H}$ constant and only correcting the surface, exactly the same effect occurs but with a drastically higher magnitude. Effectively the black-dashed curve stays under the magenta-dot-dashed curve for all damage levels and the difference vanishes around 0% and 100% tip loss.

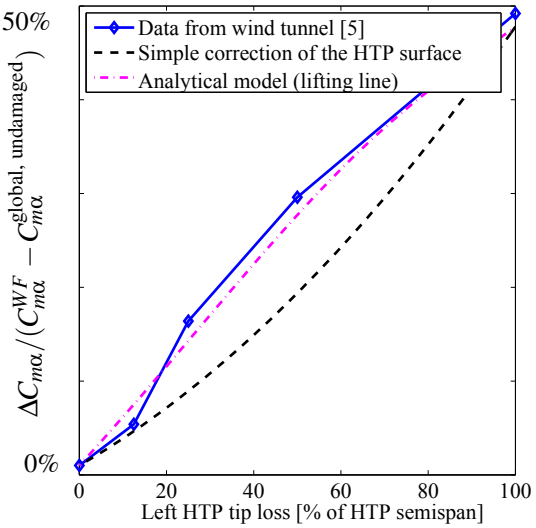

Fig. 6 Comparison Between the Wind Tunnel Results from [5] on the $C_{m\alpha}$ and the Predictions of the Lifting Line for the Damaged HTP.

The prediction made using the lifting line method matches very well the trend shown in the wind tunnel data, except for the 12.5% case. Looking at the wind tunnel data, this particular point does not seem to follow the trend defined by the other points very well. At the same time, comparing the wind tunnel and CFD results in [5] (not reproduced in the current paper) the differences are of the same order of magnitude and no "deviation" from the trend of the other points was predicted by the CFD. This leads to the conclusion that the most probable explanation is that this point was subject to some experimental uncertainty in the wind tunnel test. Whatever the explanation would be, both the CFD results of [5] and the lifting line theory have permitted to predict with good (and largely sufficient) precision the variations of the $C_{m\alpha}$ with damage level.

Note that in this comparison with wind tunnel data, it was not necessary to compute the downwash and the zero lift angle of attack because only an α-derivative was computed. The downwash gradient $\partial\varepsilon_H/\partial\alpha$ induced an additional scaling factor on the $C_{m\alpha}$, which was part of the scaling factor that had to be estimated. Besides, the HTP zero lift angle of attack only influences the constant term C_{m0} but not the $C_{m\alpha}$.

Before applying Eq. (29) to model damage to the HTP for the FMTA, the fact that the value of $C_{L\alpha}^{H}$ of the nominal (undamaged) HTP of the FMTA can be used to check the consistency between the formula of Eq. (29) and the nominal model. In order to obtain the same $C_{L\alpha}^{H}$ with this formula (given all geometric parameters) an Oswald factor of 0.75 must be used, which is a rather plausible value. Consequently, the $C_{L\alpha}^{H}$ is directly computed with the formula of Eq. (29) using this value and adjusting the geometrical parameters depending on the degree of damage. A varying value (e.g. depending on the Mach number) could be taken, but would not lead to a significant change in terms of aircraft dynamical behavior.

3.4 Downwash Gradient Determination and Engine Influence

The downwash gradient term $\partial\varepsilon_H/\partial\alpha$ can be identified from flight tests and from dynamical wind tunnel tests. It should however be noticed that handbook methods exist to model the downwash gradient, see for instance [13, 16, 22]. The level of precision provided by these handbook methods is not known to the authors.

For some aircraft a good model of the engine influence on the flow field induced by the airframe (wing, fuselage, etc.) must be identified. Of course most propeller aircraft need such a model, but not only propeller aircraft might exhibit this type of interaction: for instance, the ATTAS (VFW-614) engine blast strongly influences the induced downwash at the HTP position. This dependence of the induced downwash on engine thrust level also affects the aircraft trim conditions as well as the response to thrust changes. For the FMTA, this influence of the engines on the downwash and on the wing-fuselage derivatives had already been modeled during th MiTra-Por I project using 3D-RANS-CFD simulations

provided by colleagues of the Institute of Aerodynamics and Flow Technology. It was assumed that no change in the downwash model was required by the introduction of empennage damages.

3.5 Characteristics of the wing-fuselage configuration

The angle of zero lift and the $C_{L\alpha}^{WF}$ (i.e. for the configuration without empennage) can be obtained from the wind tunnel tests and are respectively $\alpha_0^{WF} \approx -0.6^\circ$ and $C_{L\alpha}^{WF} \approx 5.22$. If such data were not available, these terms can easily be identified from flight test data with the appropriate dynamic pitch maneuvers.

Wing geometries are usually significantly more complex than HTP geometries: the simplified methods that are able to predict α_0^H are therefore not expected to provide sufficiently precise estimates for the angle of zero lift of the wing. Additionally, the contribution of fuselage to α_0^{WF} is usually not negligible. No handbook method enabling the estimation of α_0^{WF} with acceptable precision is known to the authors. Note that once the HTP properties are determined (α_0^H and $C_{L\alpha}^H$), it should be possible to identify the two remaining parameters α_0^{WF} and $\partial\varepsilon_H/\partial\alpha$ from flight test data. However, this affirmation is however kept with a conditional as no practical demonstration is known to the authors. For the identification of the thrust influence, the flight test procedure has to be repeated several times with various thrust levels and dynamic thrust variations should be performed.

4 Conclusions and outlook

In this paper, an extension of the classical longitudinal flight dynamic derivative-based model structure was presented with the aim of easing the integration of HTP damage models in a classical airplane flight dynamic model. In addition to that, a practical and easy way to obtain the required parameter values for this model is presented. The methods used for that are known since a very long time by the aerodynamicists, but often not exploited for the derivation of airplane flight dynamic models. Consequently, this part of the paper is not about some new aerodynamics results, but aims to remind that these methods exist and constitute a very good complement to the extended derivative model structure proposed in this paper. Any kind of airplane derivative model could be extended as proposed if the HTP is not twisted and its airfoil is known, which is usually the case. For more complex HTP geometries, the same model structure can be used, but HTP aerodynamic parameter identification will require other means.

The complete model equations (with a complete empennage model and lateral equations also) following the two-part concept introduced briefly in this paper will be published in the near future. This model will also be used for fault detection, isolation and reconfiguration and fault-tolerant flight control systems research.

References

[1] Raab, C., Flugmechanisches Gesamtmodell für ein zukünftiges Militärtransportflugzeug, Version 2.0. *DLR Internal report - IB 111-2009/03*, 2009.

[2] Jann, T., Coupled simulation of cargo airdrop from a generic military transport aircraft. *AIAA Aerodynamic Decelerator System Technology Conference*, Dublin, Ireland, May 23-26, 2011, AIAA 2011-2566.

[3] Jordan, T. L., Langford, W. M., Belcastro, C. M., Foster, J. M., Shah, G. H., Howland, G., Kidd, R., Development of a Dynamically Scaled Generic Transport Model Testbed for Flight Research Experiments. *AUVSI Unmanned Unlimited*, Arlington, VA, USA, 2004.

[4] Shah, G. H., Aerodynamic Effects and Modeling of Damage to Transport Aircraft. *AIAA Atmospheric Flight Mechanics Conference*, Honolulu, HI, USA, Aug. 18-21, 2008, AIAA 2008-6203.

[5] Frink, N. T., Pirzadeh, S. Z., Atkins, H. L., Viken, S. A., Morrison, J. H., CFD assessment of aerodynamic degradation of a subsonic transport due to airframe damage. *AIAA Aerospace*

Science Meeting, Orlando, FL, USA, Jan. 4-7, 2010, AIAA 2010-500.

[6] Djellal, S., Azzam, T., On the aerodynamics of the battle damaged wings. *47th Internation Symposium of Applied Aerodynamics*, AAAF, Paris, France, March 26-28, 2012.

[7] Kim, J., Palaniappan, K., Menon, P. K., Rapid estimation of impaired aircraft aerodynamic parameters. *Journal of Aircraft*, Vol. 47, No. 4, pp.1216-1228, Jul.-Aug. 2010.

[8] Geisbauer, S., Untersuchung des Einflusses generischer Vorderkantenbeschädigungen auf die aerodynamische Leistungsfühigkeit von Flugzeugprofilen. *DLR Internal report - IB 124-2012/903*, 2012.

[9] El Al Flight 1862. Nederlands Aviation Safety Board, *Aircraft accident report 92-11*, Feb. 1994. .

[10] Mönnich, W., Ein 2-Punkt-Aerodynamikmodell für die Identifizierung. In: *Systemidentifikation in der Fahrzeugdynamik: Symposium des Sonderforschungsbereiches SFB 212 "Sicherheit im Luftverkehr"*, Braunschweig, Germany, March 10-11, 1987, DFVLR Mitteilung 87-22, ISSN: 0176-7739.

[11] Jategaonkar, R. V., *Flight vehicle system identification*. AIAA, 2006, ISBN: 1-56347-836-6.

[12] Etkin, B., *Dynamics of atmospheric flight*. John Wiley & Sons, 1972, ISBN: 0-471-24620-4.

[13] Etkin, B., *Dynamics of flight - stability and control*. 3rd Ed., John Wiley & Sons, 1996, ISBN: 0-471-03418-5.

[14] Phillips, W. F., *Mechanics of flight*. John Wiley & Sons, 2004, ISBN: 0-471-33458-8.

[15] Cook, M. V., *Flight dynamics principles*. 2nd Ed., Elsevier, 2007, ISBN: 978-0-7506-6927-6.

[16] Schmidt, D. K., *Modern flight dynamics*. MacGraw-Hill, 2010, ISBN: 978-0-07-339811-2.

[17] Brockhaus, R., Alles, W., Luckner, R., *Flugregelung*. 3rd Ed.. Springer, 2011, ISBN: 978-3-642-01442-0.

[18] Anderson, J. D., *Fundamentals of aerodynamics*. 4th Ed., MacGraw-Hill, 2007, ISBN: 007-125408-0.

[19] Munk, M. M., The determination of the angles of attack of zero lift and zero moment, based on Munk's integrals. *NACA Report No. 191*, 1924.

[20] Pankhurst, R. C., A method for the rapid evaluation of Glauert's expressions for the angle of zero lift and the moment at zero lift. British ARC, *R. & M. No. 1914*, 1944.

[21] Abbott, I. H. and von Doenhoff, A. E., *Theory of wing sections - including a summary of airfoil data*. 2nd Ed., Dover Publications, 1959, ISBN: 978-0-486-60586-9.

[22] Hoak, D. E., et al., *USAF Stability and Control DATCOM*. Wright-Patterson Air Force Base, OH, USA, AFWAL-TR-83-3048, Oct. 1960 (Revised 1978).

Copyright Statement